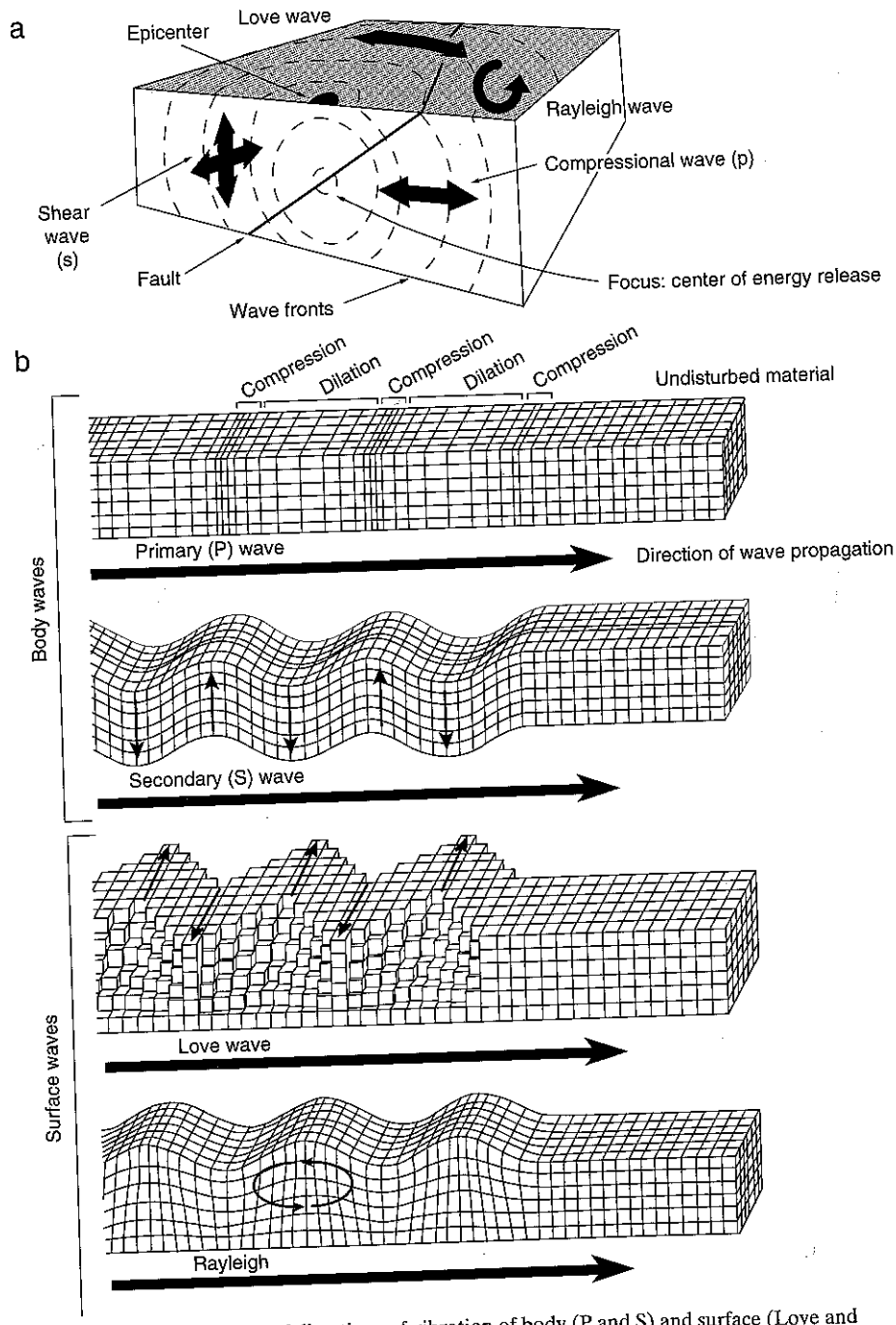

Figure 1.13 (a) Diagram of directions of vibration of body (P and S) and surface (Love and Rayleigh) waves generated by an earthquake associated with the illustrated fault. Also shown are the focus (center of energy release) and epicenter of the earthquake event. (b) Propagation of body and surface waves. (Part (a) From Hays, 1981 (13); Part (b) after Bolt, 1993 [10].)

vibration that may coincide with earthquake frequencies. Shaking of buildings is amplified when the frequency of earthquake waves is close to the natural frequency of the building. Low buildings have a higher natural frequency than taller buildings and, as a result, compressional and shear waves with relatively high frequencies tend to accentuate damage to low buildings. On the other hand, surface waves with lower frequencies tend to damage tall buildings.

High-frequency waves attenuate (die or diminish) much more quickly with distance from a generating earthquake than do low-frequency waves. Thus, tall buildings may be damaged at relatively long distances (up to several hundred kilometers) by large earthquakes [10, 13], whereas low buildings tend to sustain the greatest damage near earthquake epicenters. This principle was dramatically illustrated in 1985 when a M_W 8.1 earthquake several hundred kilometers away from Mexico City damaged or destroyed many of the taller buildings in the city.

MATERIAL AMPLIFICATION

Earth materials such as bedrock, sand and gravel, and silts and muds respond differently to seismic shaking. For example, the intensity of shaking of unconsolidated sediments may be much more severe than for bedrock (Figure 1.14). This effect is called **material amplification**. A major lesson from the 1985 earthquake affecting Mexico City was that buildings constructed on materials likely to amplify seismic shaking are extremely vulnerable to earthquakes, even if the event is centered several hundred kilometers away. Seismic waves from this earthquake, which occurred offshore of Mexico, initially contained many different frequencies, but the seismic waves that survived the several-hundred-kilometer journey to the city were those with relatively long periods of 1 to 2 s (frequencies of 1.0 to 0.5 Hz). It is speculated that when these waves struck the lake beds on which Mexico City is built, the amplitude of shaking may have increased at the surface by a factor of 4 to 5 times (Figure 1.15). The intense regular shaking caused buildings to sway back and forth, and eventually many of them collapsed or "pancaked" as upper stories collapsed onto lower ones. Most of the damage was to buildings with 6 to 16 stories, because these buildings had a natural frequency that nearly matched that of the arriving seismic waves [14].

The potential for amplification of surface waves to cause damage was again demonstrated with tragic results during the 1989 M_W 7.2 Loma Prieta (San Francisco) earthquake, when the upper tier of the Nimitz Freeway in Oakland, California, collapsed,

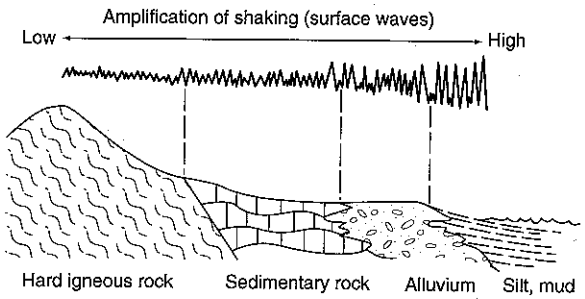

Figure 1.14 Generalized relationship between near-surface earth material and amplification of shaking during a seismic event.

a

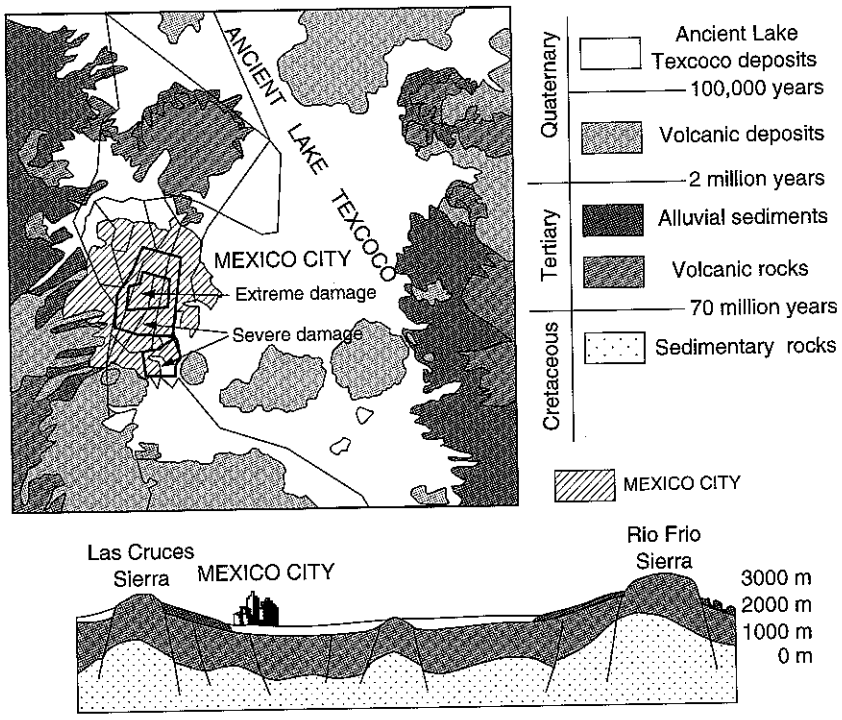

b

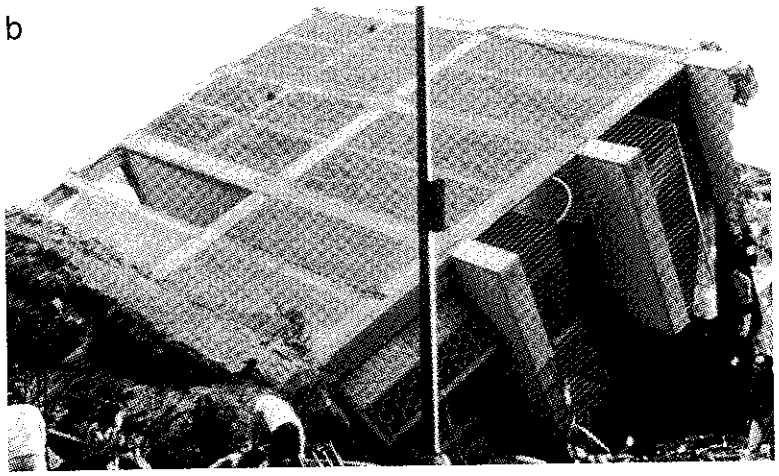

Figure 1.15 Earthquake damage, Mexico City, 1985. (a) Generalized geologic map of Mexico City showing ancient lake deposits where greatest damage occurred. (b) Multistory building, one of many that collapsed. (Map and photo courtesy of T. C. Hanks and D. Herd, U.S. Geological Survey.)

killing 41 people (Figure 1.16). Collapse of the tiered freeway occurred on a section of roadway constructed on bay fill and mud. Where the freeway was constructed on older, stronger alluvium, less shaking occurred and the structure survived. Extensive damage was also recorded in the Marina District of San Francisco (Figure 1.17), primarily in areas constructed on bay fill and mud, including debris dumped into the bay during the cleanup following the 1906 earthquake [15].

DIRECTIVITY

An earthquake may be considered as a process of rupture that starts from an initial point on the fault plane (the focus). Fault rupture does not occur instantaneously and it does not proceed in a uniform manner along the fault plane. For example, during the Northridge M_W 6.7 event, the earthquake ruptured the fault plane for approximately 8 seconds, during which time the earthquake the rupture propagated up and along the fault plane in a northwesterly direction at a speed of approximately 3 km/s. This process is known as **directivity**. The average slip across the fault was about 1 m, but the rupture propagation was not uniform and some parts of the fault plane experienced little or no slip while others experienced more than 3 m. Areas along the fault plane where slip changes are known as **asperities** and are the sources of pulses of earthquake energy that arrive at the surface at different times [16].

Directivity increases the amplitude of seismic waves in the direction of fault rupture. As a result the direction of rupture can greatly affect the intensity of seismic shaking (Figure 1.18). In the direction of propagation of fault rupture, the amplitude of the resultant wave may be as much as 10 times the amplitude of the waves in the reverse direction. This suggests that damages from seismic shaking may be much greater in the direction of fault rupture (propagation) than in the opposite direction (Figure 1.19).

ACTIVE FAULT ZONES

Most geologists would consider a fault to be **active** if it has moved during the past 10 ky[1] (Holocene Epoch). The Quaternary Period (the past 1.65 M.y.) is the most recent period of geologic time, and most of our landscape has been produced during that time. Any fault that has moved during the Quaternary Period may be classified as **potentially active** (Table 1.4). Faults that have not moved during the past 1.65 M.y. are generally classified as **inactive**. However, it is often difficult to prove the activity of a fault in the absence of historical earthquakes. To prove that a fault is active, it is necessary to determine its past earthquake history (paleoseismicity) based on the geologic record. This involves identifying faulted earth materials and determining when the most recent displacement occurred. The preceding definition of an active fault is used in the state of California for **seismic zoning**. However, other agencies have more conservative definitions for fault activity. For example, when considering seismic safety for nuclear power plants, the U.S. Nuclear Regulatory Commission defines a fault as **capable** if the fault has moved

[1] 1 ky = 1000 yrs; 1 ka = 1 ky before present (5 ka means an age of 5,000 yrs). 1 M.y. = 1,000,000 yrs; 1 Ma = 1 M.y. before present.

a

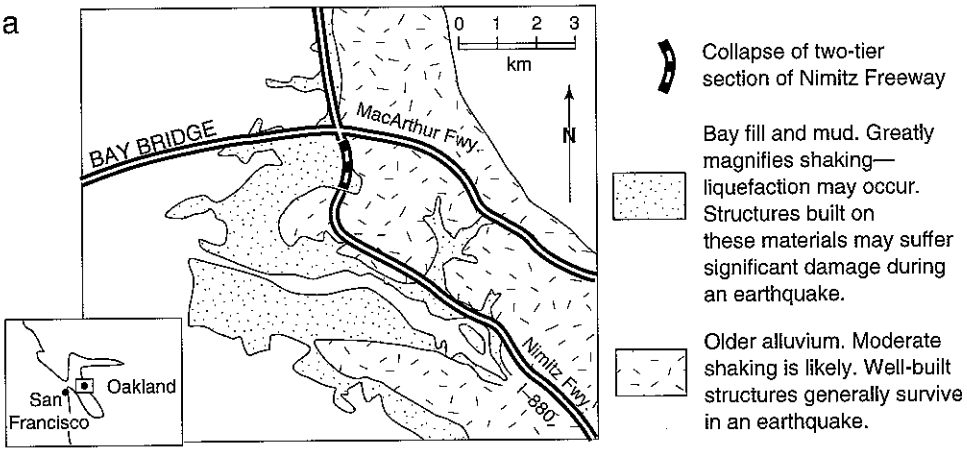

b

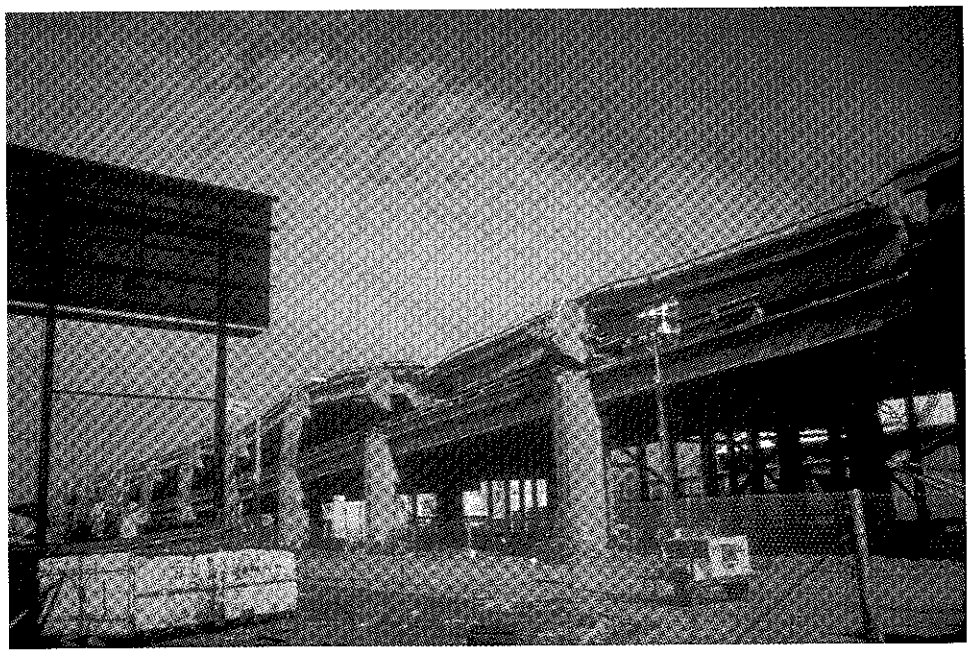

Figure 1.16 (a) Generalized geologic map of part of San Francisco Bay showing bay fill and mud and older alluvium. (b) Collapsed freeway. (Part (a) modified from Hough et al., 1990. *Nature*, 344:853–855. [copyright] Macmillan Magazines Ltd., 1990. Used by permission of the author. Part (b) courtesy of John K. Nakata, U.S. Geological Survey.)

Figure 1.17 Damage to buildings in the Marina District of San Francisco resulting from the 1989 earthquake. (Photograph courtesy of John K. Nakata, U.S. Geological Survey.)

at least once in the past 50 ky or more than once in the past 500 ky. These criteria provide a greater safety factor, reflecting increased concern for the risk of siting nuclear power plants.

SLIP RATES AND RECURRENCE INTERVALS

Our discussion of faults and earthquakes involves two important concepts: slip rates on faults, and recurrence intervals, or repeat times, of earthquakes. **Slip rate** on a fault is defined as the ratio of slip (displacement) to the time interval over which that slip occurred. For example, if a fault has moved 1 m during a time interval of 1 ky, the slip rate is 1 mm/yr (1 m/ky). The **average recurrence interval** on a particular fault is defined as the average time interval between earthquakes, and it may be determined by three methods:

1. *Paleoseismic data*: Averaging the time intervals between earthquakes recorded in the geologic record (see Chapter 8).
2. *Slip rate*: Assuming a given displacement per event and dividing that number by the slip rate. For example, if the average displacement per event is 1 m (1000 mm) and the slip rate is 2 mm/yr, then the average recurrence interval would be 500 yr.
3. *Seismicity*: Using historical earthquakes and averaging the time intervals between events.

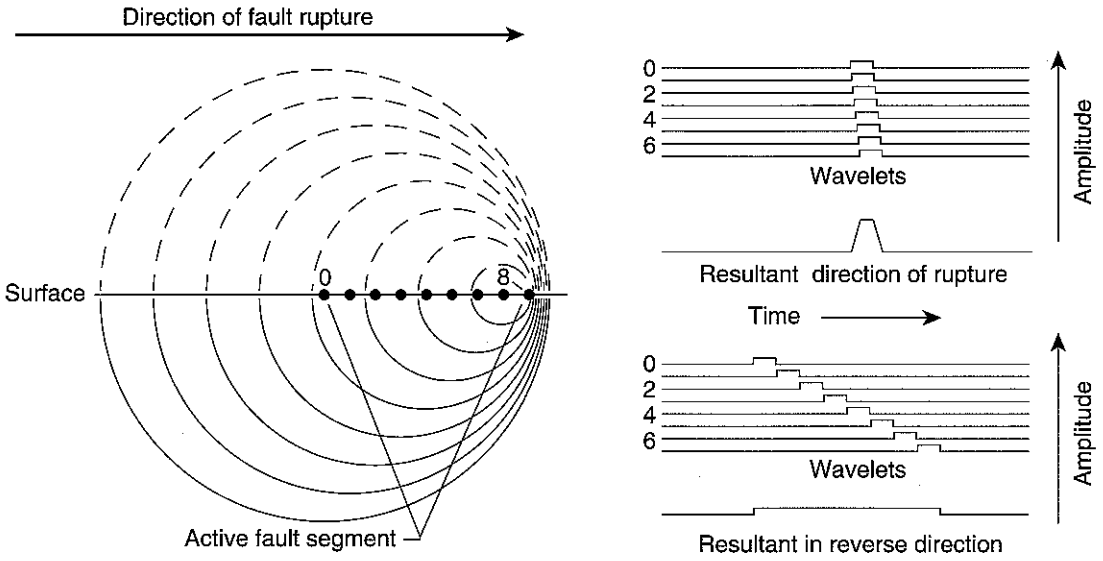

Figure 1.18 Concept of directivity increasing the amplitude of seismic waves in the direction that rupture propagates. Rupture begins at point 0, but expands asymmetrically to the right (1, 2 ... 8). Circles indicate the distance that seismic energy released at each time interval has traveled. Because the rate of rupture propagation is about equal to the speed at which the seismic waves travel, the waves from different times can coincide and amplify in areas to the right. This process is analogous to the Doppler effect of increasing pitch of sound waves from approaching train whistle. (After Benioff, 1955. *California Division of Mines Bulletin*, 171:199–202.)

Defining the terms *slip rate* and *recurrence interval* is easy, and the calculation is straightforward, but the underlying concepts are far from simple. Fault slip rates and recurrence intervals tend to be variable in time, casting suspicion on rates averaged over long periods of time. For example, it is not uncommon for earthquake events to be **clustered** in time and then be separated by relatively long periods of low activity. Both slip rate and recurrence interval will vary depending on the time interval for which data are available. The topics of slip rates and recurrence intervals will be discussed repeatedly in this book. They are introduced here to facilitate later discussions.

TECTONIC CREEP

Tectonic creep is the process of displacement along a fault zone that is not accompanied by perceptible earthquakes. The process can slowly damage roads, sidewalks, building foundations, and other structures. Tectonic creep has damaged culverts under the football stadium of the University of California at Berkeley, and periodic repairs have been necessary. Movement of approximately 3.2 cm in 11 years was measured (Figure 1.20) [17]. More rapid rates of tectonic creep have been recorded on the Calaveras fault zone, a segment of the San Andreas fault near Hollister, California. At one location, a winery located on the fault is slowly being pulled apart at about 1 cm/yr [18]. Damages resulting from tectonic creep generally occur along narrow fault zones subject to slow, continuous displacement. However, creep may also be discontinuous and variable in rate.

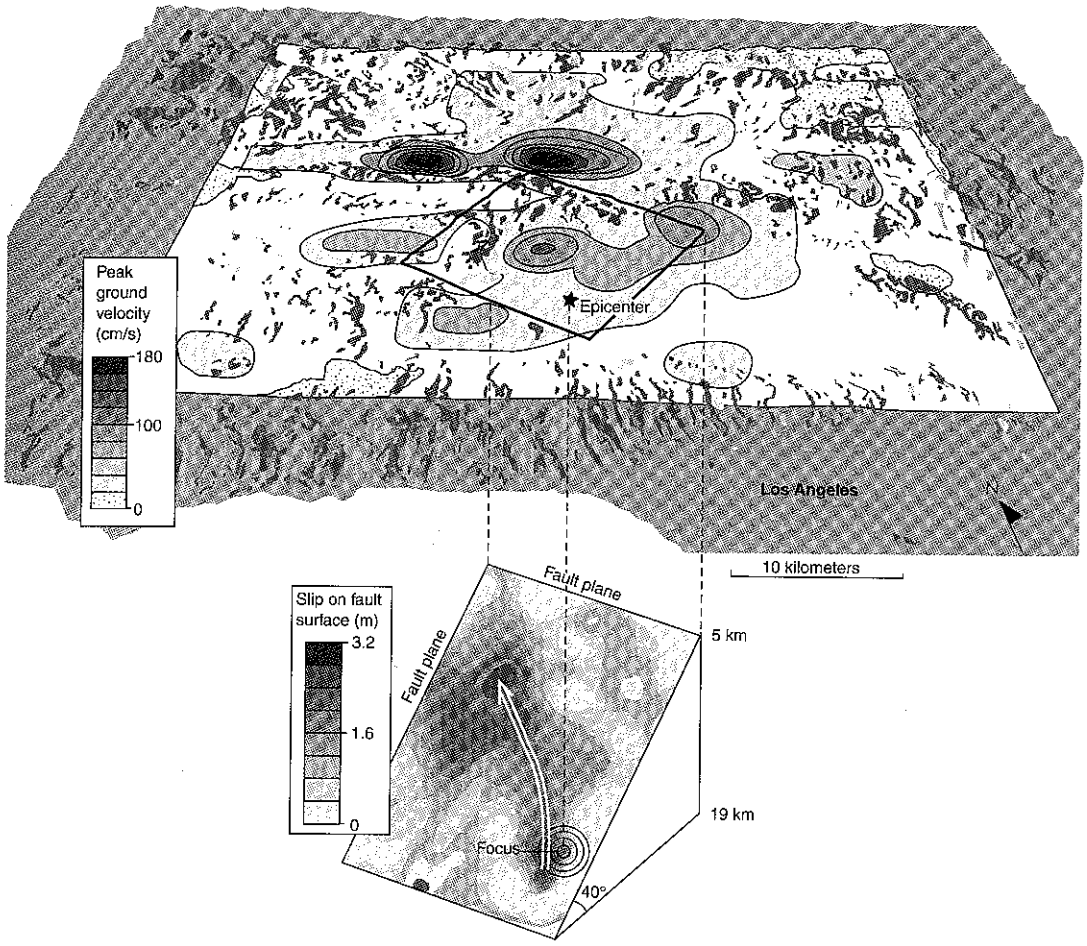

Figure 1.19 Aerial view of the Los Angeles region from the south showing the epicenter of the 1994 Northridge earthquake with peak ground motion in centimeters per second and the fault plane in its subsurface position. The fault rupture apparently began at the focus in the southeastern part of the fault plane and proceeded upward and to the northwest, as shown by the arrow. The area that ruptured is approximately 430 km^2, and the fault plane dips at approximately 40° to the south-southwest. Notice that maximum slip and peak ground velocities both occur to the northwest of the epicenter. (U.S. Geological Survey, 1996. U.S. Geological Survey Open-File Report 96–263.)

ESTIMATION OF SEISMIC RISK

Catastrophic earthquakes are devastating events. Historic earthquakes have destroyed large cities and taken thousands of lives in a matter of seconds. Table 1.5 lists some of the major historical earthquakes that have occurred in the United States.

Seismic risk maps have been prepared for the United States (Figure 1.21). One way of interpreting Figure 1.21 is that the darkest areas represent the regions of greatest seismic hazard, because those areas are most likely to experience the greatest seismic shaking (in this case, horizontal ground acceleration) in an average 50-yr interval.

Table 1.4

TERMINOLOGY RELATED TO DEGREE OF FAULT ACTIVITY.

Geologic Age			Years Before Present	Fault Activity
Era	Period	Epoch		
Cenozoic	Quaternary	Historic (Calif.) Holocene	200	Active
		Pleistocene	10,000	Potentially active
	Tertiary	Pre-Pleistocene	1,650,000	
Pre-Cenozoic time			65,000,000	Inactive
Age of the earth			4,500,000,000	

(After California State Mining and Geology Board Classification, 1973.)

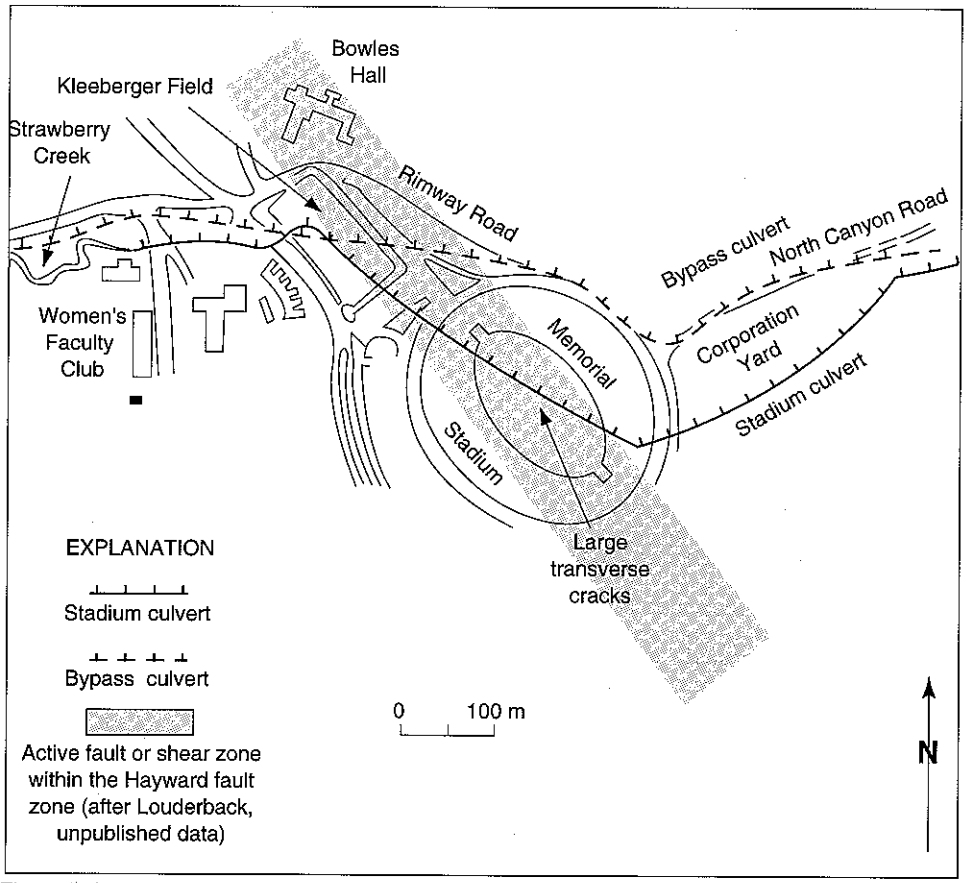

Figure 1.20 Map showing the location of the University of California at Berkeley Memorial Stadium, the active fault or shear zone within the Hayward fault zone, and the stadium culvert where major cracking has taken place. (After Radbruch et al., 1966 [17].)

Table 1.5

SELECTED MAJOR EARTHQUAKES IN THE UNITED STATES.

Year	Locality	Damage $ Million	Lives Lost
1811–12	New Madrid, Missouri	Unknown	
1886	Charleston, South Carolina	23	60
1906	San Francisco, California	524	700
1925	Santa Barbara, California	8	13
1933	Long Beach, California	40	115
1940	Imperial Valley, California	6	9
1952	Kern Country, California	60	14
1959	Hebgen Lake, Montana (damage to timber and roads)	11	28
1964	Alaska and U.S. West Coast (includes tsunami damage from earthquake near Anchorage)	500	131
1965	Puget Sound, Washington	13	7
1971	San Fernando, California	553	65
1983	Coalinga, California	31	—
1983	Central Idaho	15	2
1987	Whittier, California	358	8
1989	Loma Prieta (San Francisco), California	5,000	62
1992	Landers, California	27	1
1994	Northridge, California	40,000	61
2001	Seattle, Washington	2,000	1

(Modified after Hays, 1981 [13].)

The map is based on historical seismicity, frequency of earthquakes of various magnitudes, and slip rates on faults. Estimated ground accelerations assume firm rock conditions. Actual hazard at a particular site may vary as a result of material amplification or directivity of seismic shaking. Although regional earthquake hazard maps are valuable, considerably more data are necessary to evaluate hazardous areas more precisely in order to develop building codes and determine insurance rates.

In California, **conditional probabilities** (probability dependent on known or estimated conditions) of major earthquakes along segments of the San Andreas fault and related faults for a 30-yr period (1994–2024) have been calculated (Figure 1.22). The probabilities were calculated following synthesis of historical records and geologic evaluation of prehistoric earthquakes [19]. In 1988, this approach assigned a probability of about 30% for a major event on the San Andreas fault segment through the Santa Cruz Mountains, where the M_W 7.2 Loma Prieta earthquake occurred on October 17, 1989. Occurrence of this earthquake supports the validity of the conditional-probability approach. The probability of a large earthquake on the southern segment of the San Andreas fault is estimated to be close to 50% for the next 30 years. The M_W 7.6 Landers earthquake that occurred east of the San Andreas fault in 1992 was a surprising event. That event produced major right-lateral horizontal surface displacement of up to 5 m, and maximum Modified Mercalli intensity of VIII [20] on a fault system that was previously mapped but that had not received much attention. This large earthquake caused relatively little damage ($27 million) and one death, primarily because it occurred in a region with low buildings and few people.

Another large (M_W 7.1) right-lateral strike-slip earthquake, known as the Hector Mine earthquake, occurred in a sparsely populated part of the Mojave Desert about 40

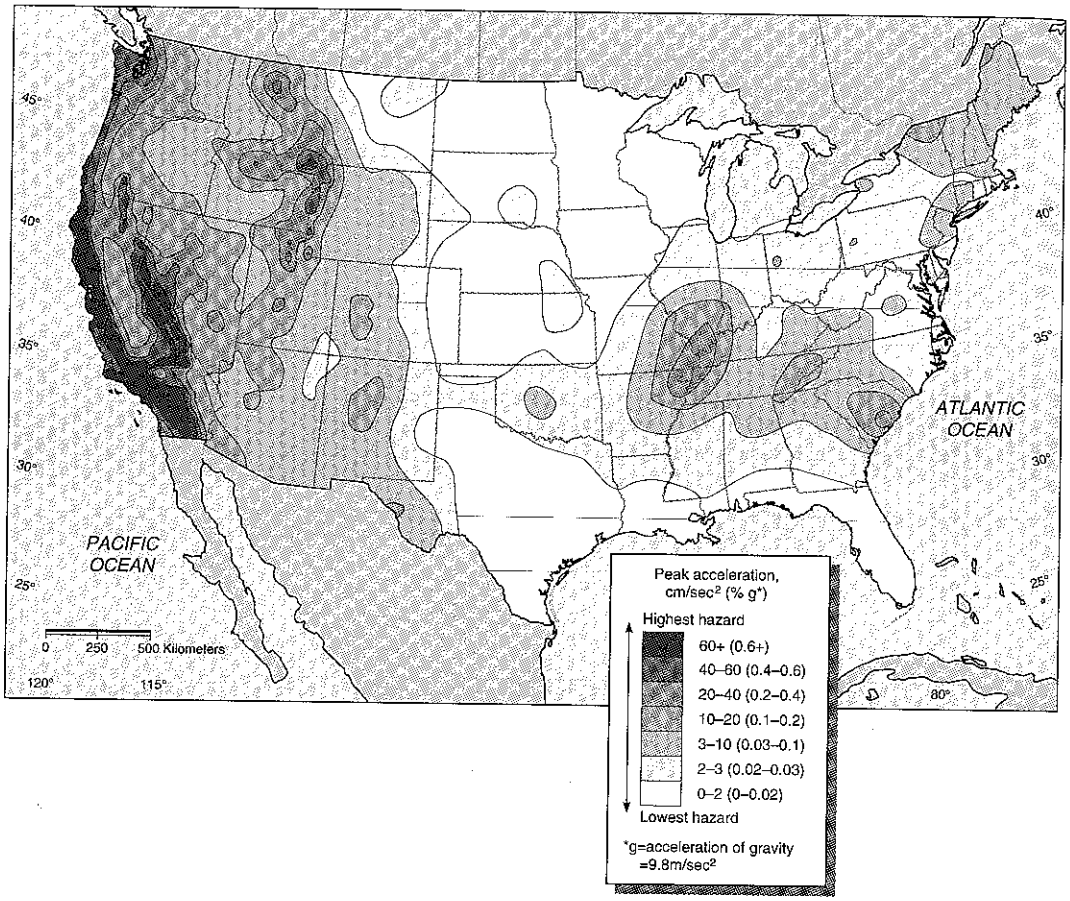

Figure 1.21 A probabilistic approach to the seismic hazard from ground shaking in the United States, showing ground accelerations having a 10% probability of being exceeded in a 50-year time period. (From U.S. Geological Survey 1999.)

km north of Joshua Tree, California, in October of 1999. Rupture length of the event, which was on the previously mapped north-northwest trending Lava Lake fault in the eastern Mojave Shear Zone, was 40 km with maximum right-lateral displacements of 4 to 5 m. The fault was mapped years ago by Thomas Dibblee, Jr. (a famous field geologist who mapped much of California) and reinforces the value of geologic mapping in recognizing faults. The Eastern Mojave shear zone was also the source for the 1992 (M_W 7.6) Landers earthquake. The shear zone evidently relieves some of the strain that builds up on the boundary between the North American and Pacific Plates. However, most strain is thought to be relieved along the boundary by the San Andreas fault system. It is speculated that Hector Mine (1999) and Landers (1992) events along with smaller events may represent a clustering of earthquakes. That is, the shear zone may produce several events within a relatively short time period of decades to a hundred or so years followed by several thousands years of seismic quiescence [21]. Of course, the events might be coincidental, but some connection is likely.

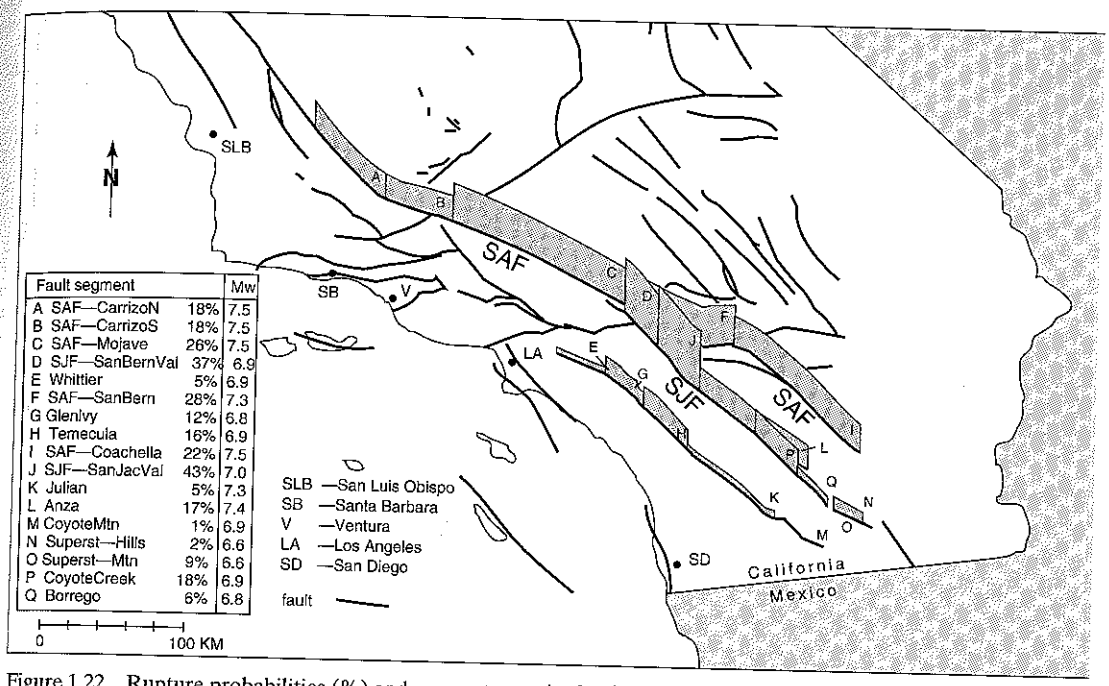

Fault segment		Mw
A SAF—CarrizoN	18%	7.5
B SAF—CarrizoS	18%	7.5
C SAF—Mojave	26%	7.5
D SJF—SanBernVal	37%	6.9
E Whittier	5%	6.9
F SAF—SanBern	28%	7.3
G Glenlvy	12%	6.8
H Temecula	16%	6.9
I SAF—Coachella	22%	7.5
J SJF—SanJacVal	43%	7.0
K Julian	5%	7.3
L Anza	17%	7.4
M CoyoteMtn	1%	6.9
N Superst—Hills	2%	6.6
O Superst—Mtn	9%	6.6
P CoyoteCreek	18%	6.9
Q Borrego	6%	6.8

Figure 1.22 Rupture probabilities (%) and moment magnitudes (M_W) for the time period 1994 to 2024 for fault segments associated with the San Andreas fault (SAF), San Jacinto fault (SJF), and other related faults (listed) associated with SAF. (Modified after Working Group on California Earthquake Probabilities, 1995. Bulletin of the Seismological Society of America, 85:379–439.)

As more historical and geologic information is gathered, more detailed estimation of the probability of future earthquakes is possible. For example, based on research since the Loma Prieta (San Francisco) earthquake, it has been estimated for the San Francisco Bay region that at least one major earthquake with M_W 6.7 or larger has a 70 ± 10% probability of occurring between 2000 and 2030 [22]. Such an event is capable of causing widespread destruction and loss of life. If the event is centered in a highly urbanized area, damages and loss of life could, in a worst-case scenario, be similar to the M_W 6.9 event that occurred in Kobe, Japan, in 1995, which killed more than 6000 people and caused damages of about $100 billion. A M_W 6.7 event was assumed in the probability analysis because that is the magnitude of the 1994 Northridge (Los Angeles) earthquake, which caused 61 deaths and more than $40 million in damage.

Earthquake probabilities for specific faults for one or more M_W 6.7 events from 2000 to 2030 are shown on Figure 1.23. The 70 ± 10% probability for a large damaging earthquake in the San Francisco Bay region in the next 30 years was derived by analyzing several processes [22]:

- Motion of the Pacific and North American tectonic plates
- Slip on faults that mostly occur during earthquakes
- How strain from current plate motion of 3.8 cm/yr (measured from Global Positioning System, GPS; see Chapter 3) is distributed into the individual faults in the region

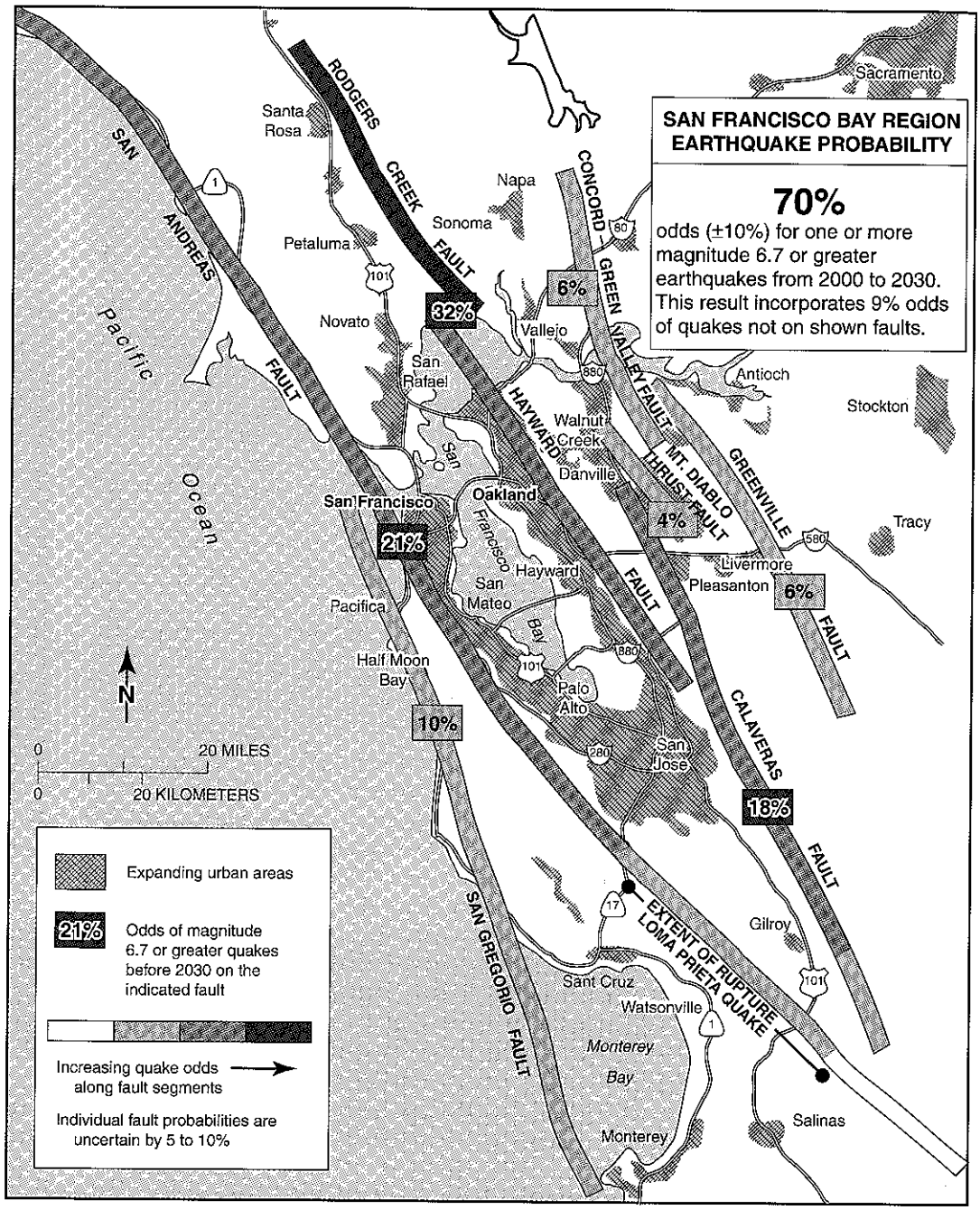

Figure 1.23 Probability of at least one M_W 6.7 or greater earthquake occurring from 2000 to 2030 on specific faults in the San Francisco Bay region. Probability of 70 ± 10% is the combined probability for the entire region and is not the simple sum of individual probabilities for faults shown. (Working Group on California Earthquake Probabilities, 1999. U.S. Geological Survey Fact Sheet 152–99.)

uakes

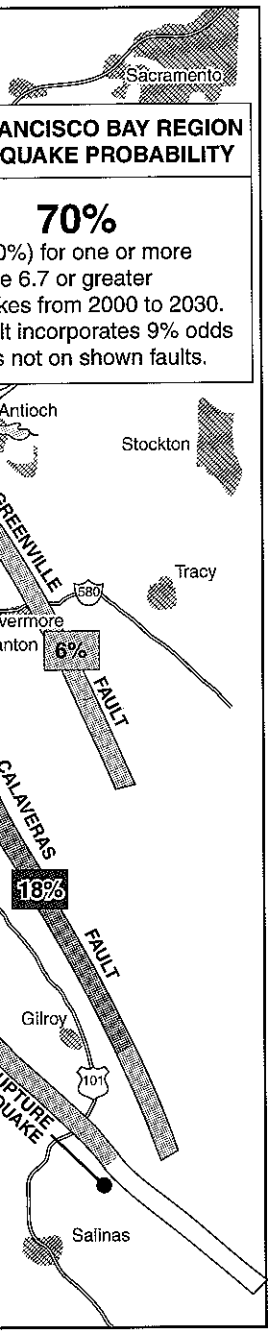

000 to 2030 on specific faults in
he entire region and is not the
Earthquake Probabilities,

- Slip on fault that does not accompany earthquakes, known as tectonic creep (discussed previously)

Results of the San Francisco Bay region study emphasize the importance for all communities in the region to continue to prepare for earthquakes [22].

EFFECTS OF EARTHQUAKES

Primary effects of earthquakes are caused directly by the earthquake and can include violent ground-shaking motion accompanied by surface rupture and permanent displacement. For example, the M_W 7.7 1906 earthquake at San Francisco produced 6.5 m of horizontal displacement and a maximum Modified Mercalli intensity of XI [10]. Such violent motions can produce surface accelerations that snap and uproot large trees and knock people to the ground. This motion may shear or collapse large buildings, bridges, dams, tunnels, and pipelines, as well as other rigid structures [23]. The great 1964 Alaskan earthquake (M_W 9.2) caused extensive damage to railroads, airports, and buildings. The 1989 Loma Prieta (San Francisco) earthquake, with a M_W 7.2, was much smaller than the Alaska event and yet caused about $5 billion in damage. The 1994 Northridge earthquake, with M_W 6.7, was one of the most expensive disasters ever in the United States. The Northridge event caused so much damage because there was so much there to be damaged—the Los Angeles region is highly urbanized and has a high population density.

Short-term secondary effects of earthquakes include liquefaction, landslides, fires, seismic seawaves (tsunami), and floods (following collapse of dams). Long-term secondary effects include regional subsidence or emergence of landmasses and regional changes in groundwater levels.

LIQUEFACTION

Liquefaction is defined as the transformation of water-saturated granular material from a solid to a liquid state. During earthquakes, this may result from an increase in porewater pressure caused by compaction during intense shaking. Liquefaction of near-surface water-saturated silts and sand causes the materials to lose shear strength and flow. As a result, buildings may tilt or sink into the liquefied sediments, and tanks or pipelines buried in the ground may float to the surface [24].

LANDSLIDING

Intense earthquake shaking commonly triggers landslides (a comprehensive term for several types of hillslope failure) in hilly and mountainous areas. Landslides can be extremely destructive and cause great loss of life, such as during a M_W 7.7 1970 earthquake in Peru. In that event, more than 70,000 people died; of this total, 20,000 were killed by a giant landslide that buried several towns. Both the 1964 Alaskan earthquake and the 1989 Loma Prieta earthquake caused extensive landslide damage to buildings, roads, and other structures.

FIRE

Fire is a major secondary hazard associated with earthquakes. Shaking of the ground and surface displacements can break electrical power and gas lines and ignite fires. In individual homes and other buildings, appliances such as gas heaters may be knocked over. The threat from fire is doubled because firefighting equipment may be damaged and water mains may be broken. Earthquakes in both Japan and the United States have been accompanied by devastating fires. The San Francisco earthquake of 1906 has been called the "San Francisco Fire"; in fact, 80% of the damage from that event was caused by firestorm that ravaged the city for several days. The 1989 Loma Prieta earthquake also caused large fires in the city's Marina District. Perhaps the most lethal earthquake-induced fire occurred in 1923 in Japan. The earthquake killed 143,000 people, and 40% of them died in a firestorm that engulfed an open space where people had gathered in an unsuccessful attempt to reach safety [23]. The 1995 M_W 6.9 Kobe, Japan, earthquake ruptured gas lines, and fires devastated parts of the city. Ruptured water lines and damaged roads prevented firefighters from reaching and extinguishing fires.

TSUNAMI

Tsunami, or seismic sea waves, can be extremely destructive and present a serious natural hazard. Most of the lives lost in the 1964 Alaskan earthquake were attributed to tsunami (Figure 1.24). Fortunately, damaging tsunami occur infrequently and are usually

Figure 1.24 Tsunami damage to fishing boats at Kodiak, Alaska, caused by the 1964 earthquake. (Photograph courtesy of National Oceanic and Atmospheric Administration [NOAA].)

confined to the Pacific Basin. The frequency of these events in the United States is about one every 8 years [25]. Tsunami originate when ocean water is vertically displaced during large earthquakes, submarine mass movements, or submarine volcanic eruption. In open water the waves may travel at speeds as great as 800 km/h, and the distance between successive crests may exceed 100 km. Wave heights in deep water may be less than 1 m, but when the waves enter shallow coastal waters they slow to less than 60 km/h, and their heights may increase to more than 20 m.

A small town on the island of Okushiri, Japan, was extensively damaged from the July 12, 1993, tsunami produced by an M_W 7.8 earthquake in the Sea of Japan. Vertical run-up (elevation above sea level to which water from the waves reached) varied from 15 m to 30 m [26]. There was virtually no warning because the epicenter of the earthquake was very close to the island and the big waves arrived only 2 to 5 minutes after the earthquake. The tsunami killed 120 people and caused $600 million in property damage.

A magnitude M_W 7.1 earthquake on July 17, 1998, with an epicenter located 50 km off the coast of Papua New Guinea, caused a large tsunami with wave heights 10 to 15 m. A series of three waves arrived 10 to 20 minutes after the earthquake, killing over 2100 people. The wave height and run-up on shore was surprisingly high for a subduction zone earthquake of M_W 7.1. The tsunami probably resulted from a combined effect of the earthquake and a submarine landslide. The Papua New Guinea event emphasizes the potential devastating damage that can result from unusually large waves produced by a locally generated earthquake [27, 28].

Tsunami also can cause catastrophic damage thousands of kilometers from where they are generated. In 1960 an earthquake originating in Chile triggered a tsunami that reached Hawaii 15 hours later, killing 61 people. However, long travel times now allow many tsunami to be detected in time to warn the coastal communities in their path. Following an earthquake that produces a tsunami, the arrival time of the waves can often be estimated to within 1.5 minutes per hour of travel time. This information has been used to produce tsunami warning systems such as that shown for Hawaii in Figure 1.25.

Consideration is now being given to produce other tsunami warning systems for example, to warn residents in northwestern California of tsunami generated by Alaskan or Cascadia subduction-zone earthquakes. Travel time for a tsunami from the Aleutian Islands in Alaska to northern California is about 4 hours, and movement of the tsunami southward can be monitored from changes in water levels at coastal tide gauges. The plan involves placing such gauges on the bottom of the Pacific Ocean, four off Alaska, and three off the northwest coast of California.

The hazard from a tsunami at a particular site on the coast depends in part on local coastal and sea-floor topography, that may increase or decrease wave height [10]. Damage caused by tsunami is most severe at the water's edge, where boats, harbors and buildings, transportation systems, and utilities may be destroyed. The waves may also cause damage to aquatic and supratidal life in both near- and on-shore environments [25].

Waves caused by landslides may also have considerable effect and cause extensive damage. In 1958 an earthquake triggered a landslide into Lituya Bay, Alaska, causing a truly giant wave that produced run-up on land to an elevation of over 500 m above sea level [29].

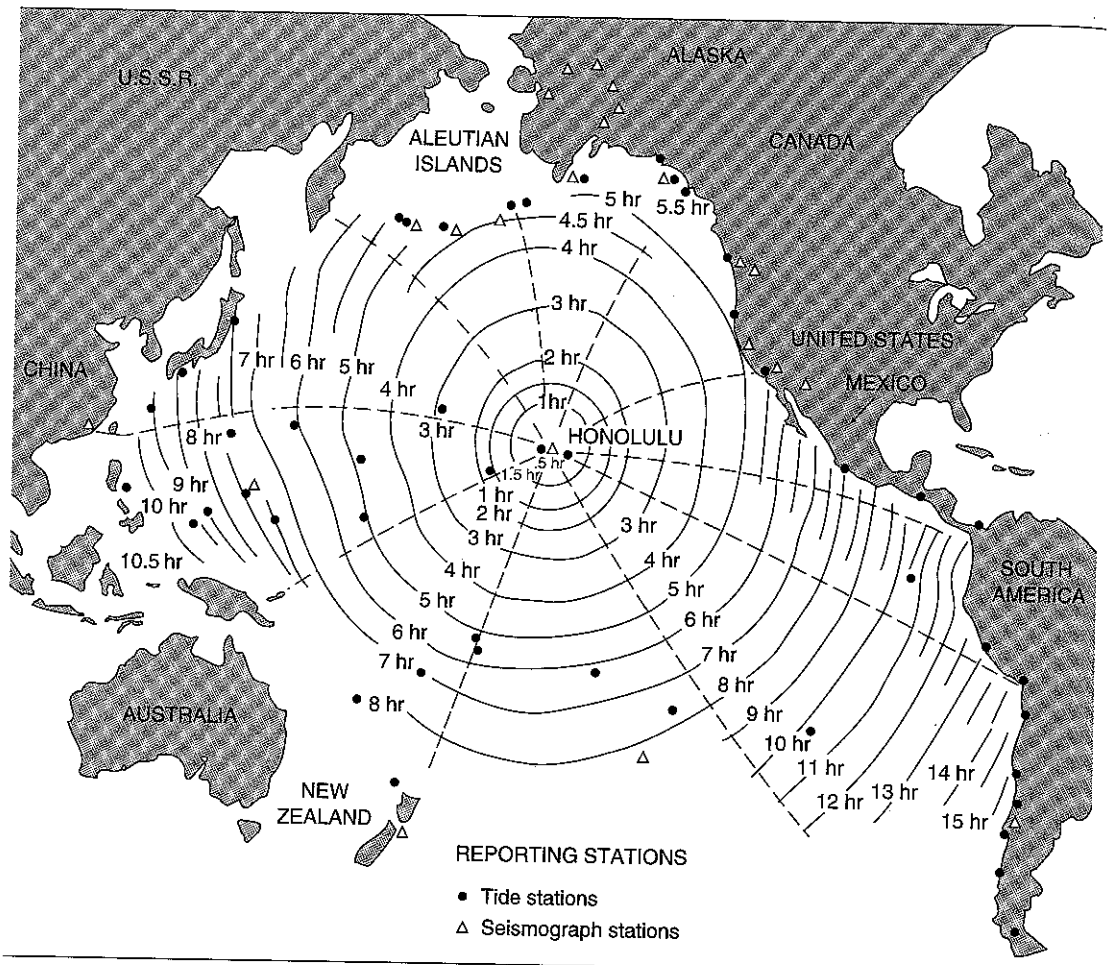

Figure 1.25 Tsunami warning system. Map shows reporting stations and tsunami travel times to Honolulu, Hawaii. (From NOAA.)

REGIONAL CHANGES IN LAND ELEVATION

Vertical deformation, including both uplift and subsidence, is another secondary effect of some large earthquakes. The great (M_W 9.2) 1964 Alaskan earthquake, with Modified Mercalli intensity of X–XI [10], caused vertical deformation over an area of more than 250,000 km^2 [30]. The deformation included two major zones of warping, each about 500 km long and more than 210 km wide (Figure 1.26), including uplift as much as 10 m and subsidence as much as 2.4 m. The effects of these regional changes in land level ranged from severely disturbing coastal marine life to changes in groundwater levels. As a result of subsidence, flooding occurred in some communities, whereas in areas of uplift, canneries and fishermen's homes were displaced above the high-tide line, rendering docks and other facilities inoperable. In 1992, a major earthquake (M_W 7.1) near Cape Mendocino in northwestern California produced approximately 1 m of uplift at the

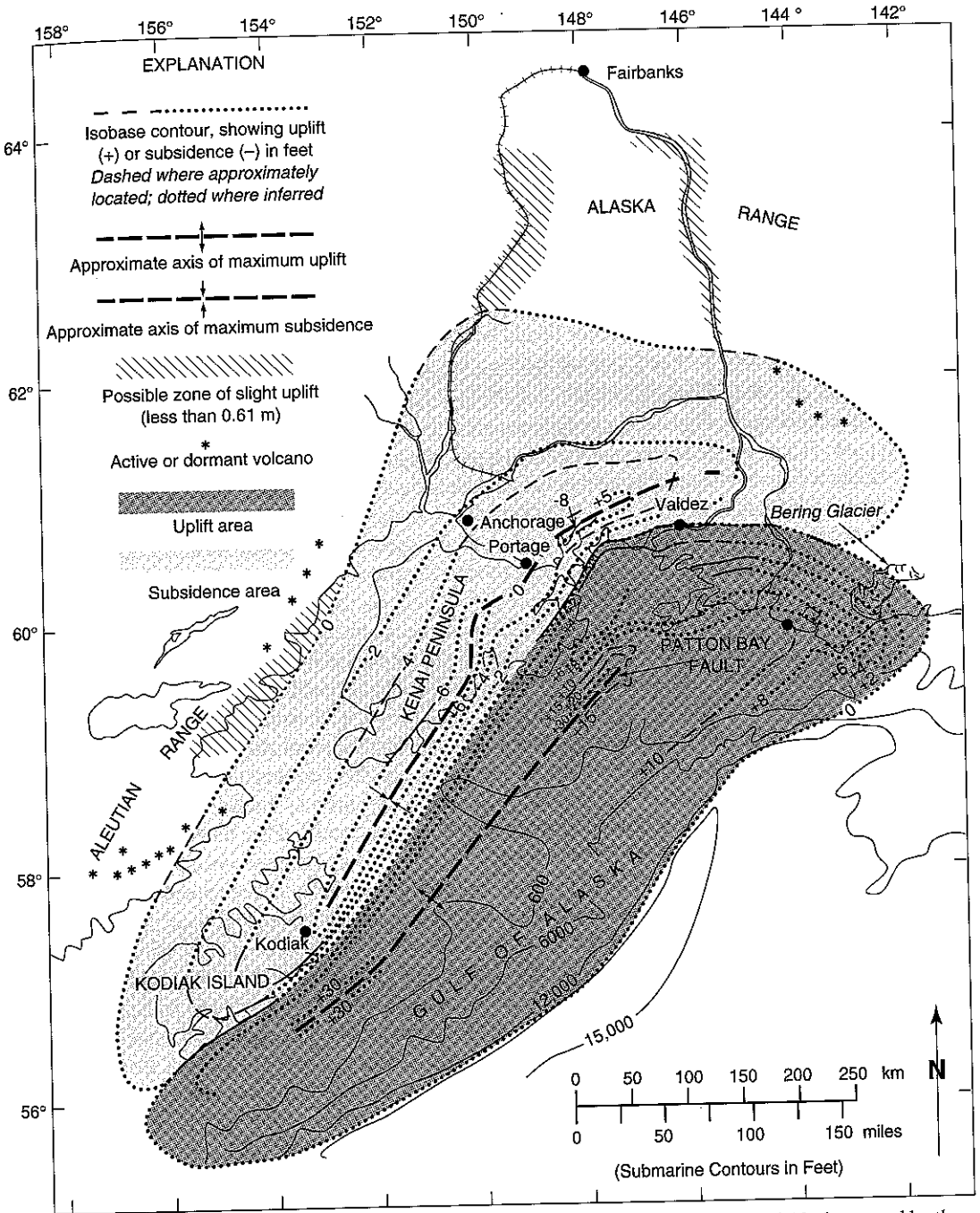

Figure 1.26 Map showing the distribution of tectonic uplift and subsidence in south-central Alaska caused by the Alaskan earthquake of 1964 (2 to 30 ft = 0.6 to 9.2 m). (From Eckel, 1970. U.S. Geological Survey Professional Paper 0546.)

shoreline, resulting in the deaths of communities of marine organisms exposed by the uplift [31] (see Chapter 6).

EARTHQUAKES CAUSED BY HUMAN ACTIVITY

Several human activities are known to cause earthquakes or to increase earthquake activity. Damage from these earthquakes is regrettable, but the lessons learned may help control or stop large catastrophic earthquakes in the future. Four ways that the actions of people can cause earthquakes are [32]:

- Loading the Earth's crust, such as a result of building dams and impounding reservoirs (reservoir-induced seismicity)
- Deep-well injection of liquid waste
- Mining that reduces confining pressure of rocks above mined areas
- Underground nuclear explosions

During the first 10 years following the completion of the Hoover Dam on the Colorado River in Arizona and Nevada, several hundred local tremors occurred. Most of these were very small, but one had a magnitude of about 5, and two had magnitudes of about 4 [32]. An earthquake—attributed to reservoir-induced seismicity—of magnitude about 6 in India killed about 200 people following dam construction and filling of a reservoir. Evidently, faults may be activated by the increased load of water on the land and by increased water pressure in the rocks below the reservoir.

From April 1962 to November 1965, several hundred earthquakes occurred in the Denver, Colorado, area. The largest earthquake had a M 4.3 and knocked bottles off store shelves. The source of the earthquakes was eventually traced to the Rocky Mountain Arsenal, which was manufacturing materials for chemical warfare. Liquid waste from the manufacturing process was being pumped down a disposal well to a depth of about 3600 m. The rock receiving the waste was a highly fractured metamorphic unit, and injection of liquid increased the fluid pressure, apparently facilitating slippage along preexisting fractures and producing the earthquakes. Study of the earthquake activity revealed a strong correlation between the rate of injection of waste and the occurrence of earthquakes. When waste injection stopped, the earthquakes stopped [33]. These induced earthquakes in the Denver area were a milestone because they alerted scientists to the fact that earthquakes and fluid pressure are related.

Other human activities, including quarrying, mining, and withdrawal of petroleum, may induce shallow small earthquakes as a result of the removal of rock or fluid. For example, in April 1995 a magnitude 2.3 earthquake was felt at a diatomite processing plant and quarry in the westernmost Transverse Ranges near the city of Lompoc, California. The earthquake was recorded on seismograph stations as far as 185 km away. Several hours later, workers at the quarry found a 210-m-long reverse-fault scarp on the floor of the quarry. Other ruptures had been reported in 1981, 1985, and 1988, and investigation of the 1995 event suggests that the earthquake was the result of the removal of approximately 40 m of overburden in the quarry. Furthermore, it was concluded that the 40 m was a critical threshold value that reduced the normal stress (weight of the overburden) necessary to induce small earthquakes. Careful evaluation of the quarry floor and surrounding area suggests that the maximum observed rupture length was about 770 m and maximum scarp height was 18 cm. The Lompoc event illustrates

co-seismic rock failure (faulting) at a scale intermediate between laboratory experiments and large damaging crustal scale earthquakes [34].

Numerous earthquakes with magnitudes as large as 5.0 to 6.3 have been triggered by underground explosions at the U.S. nuclear test site in Nevada [32]. Analysis of the aftershocks suggests that the explosions caused some release of natural tectonic strain. This led to discussions by scientists as to whether nuclear explosions might be used to prevent large earthquakes by releasing strain before it reached a critical point and caused a large earthquake. These discussions never resulted in serious consideration of actual application.

THE EARTHQUAKE CYCLE

Observations of the 1906 San Francisco earthquake led to a model known as the **earthquake cycle**. Important features of the hypothesis are related to drop in elastic strain following an earthquake and reaccumulation of strain prior to the next event. **Strain** was defined previously as deformation (displacement or change in shape or volume) resulting from stress, and **elastic strain** may be thought of as deformation that is not permanent, provided that the stress is released. If the strain is released, the deformed material returns to its original shape; for example, when a rubber band is stretched and released or when an archery bow is bent and released. During an earthquake, elastic strain drops because there is a stress drop when the rocks break and permanent displacement occurs (the rubber band or bow breaks). This process is referred to as **elastic rebound** (Figure 1.27). It takes time for sufficient elastic strain to accumulate again to produce another earthquake [12]. The earthquake cycle is discussed further in Chapter 3.

Although we have many empirical observations concerning physical changes in earth materials before, during, and after earthquakes, there is no general agreement on a physical model to explain the observations. One model, known as the **dilatancy diffusion model** [10, 35], assumes that the first stage in earthquake development is an increase of elastic strain in rocks that causes them to dilate, or undergo an inelastic increase in volume after the stress on the rock reaches one-half its breaking strength. During dilation, open fractures develop in the rocks, and at this stage, the first physical changes take place that might indicate a future earthquake. The model assumes that the dilatancy and fracturing of the rocks are first associated with a relatively low water pressure in the dilated rocks (stage 2, Figure 1.28), which helps to produce lower seismic velocity, more earth movement, higher radon gas emission (radon is a naturally radioactive gas that is dissolved in water and released as rocks fracture and dilate), lower electrical resistivity, and fewer minor seismic events. Water then enters the open fractures (stage 3, Figure 1.28), causing the pore pressure to increase (which increases the seismic velocity while further lowering electrical resistivity), thus weakening the rocks and triggering an earthquake (stage 4). After the movement and release of stress, the rocks resume many of their original characteristics (stage 5) [35].

There is considerable controversy concerning the validity of the dilatancy diffusion model. One aspect of the model gaining considerable favor is the role of **fluid pressure** (force per unit area exerted by a fluid) in earthquakes. As we learn more about rocks at seismogenic depths (the depth where earthquakes originate), it is apparent that a lot of

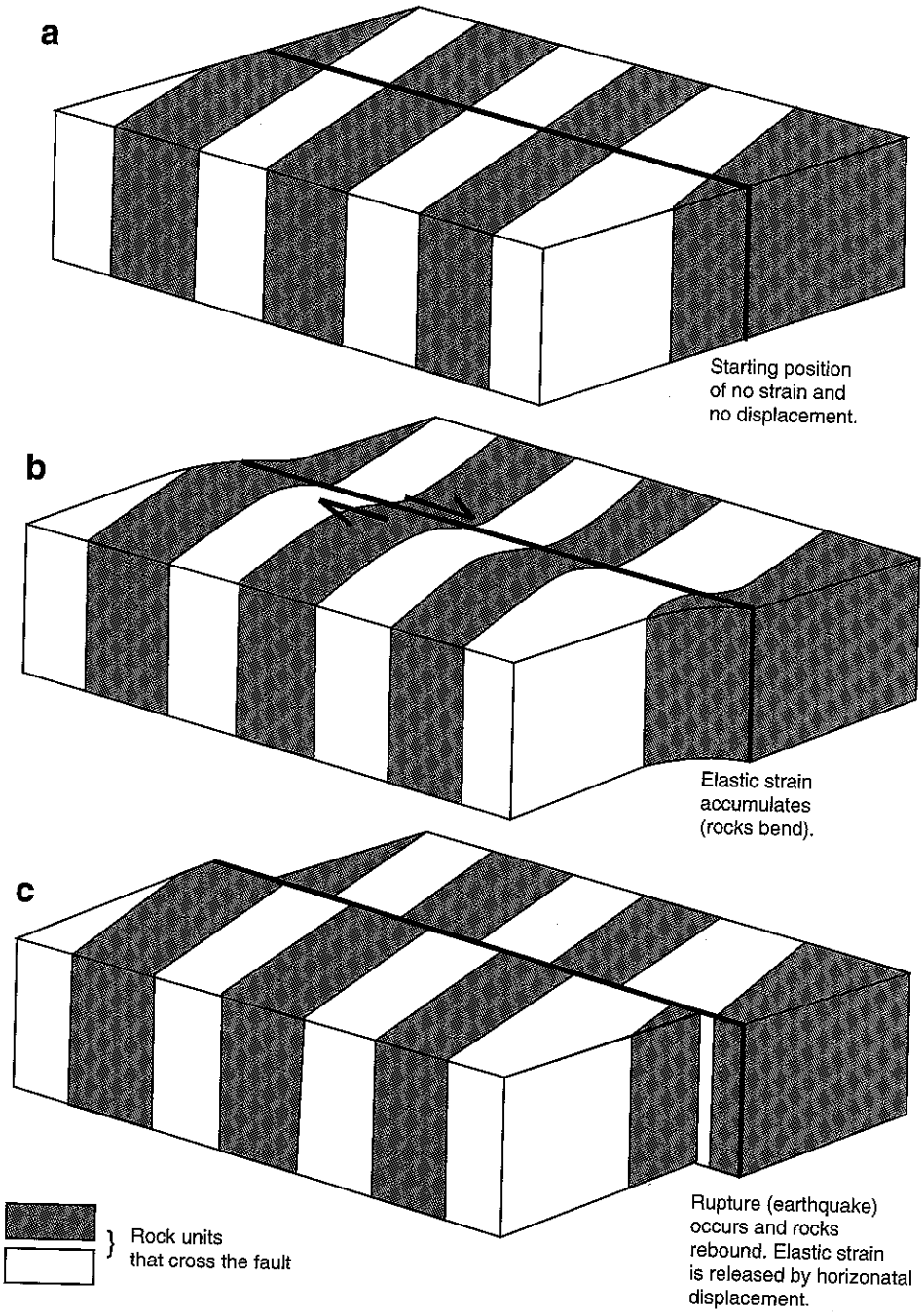

Figure 1.27 Idealized block diagrams illustrating the earthquake cycle and elastic rebound. (a) Beginning position with no strain or displacement. (b) After accumulation of elastic strain. (c) Following earthquake and rupture. (Courtesy of F. Duennebier.)

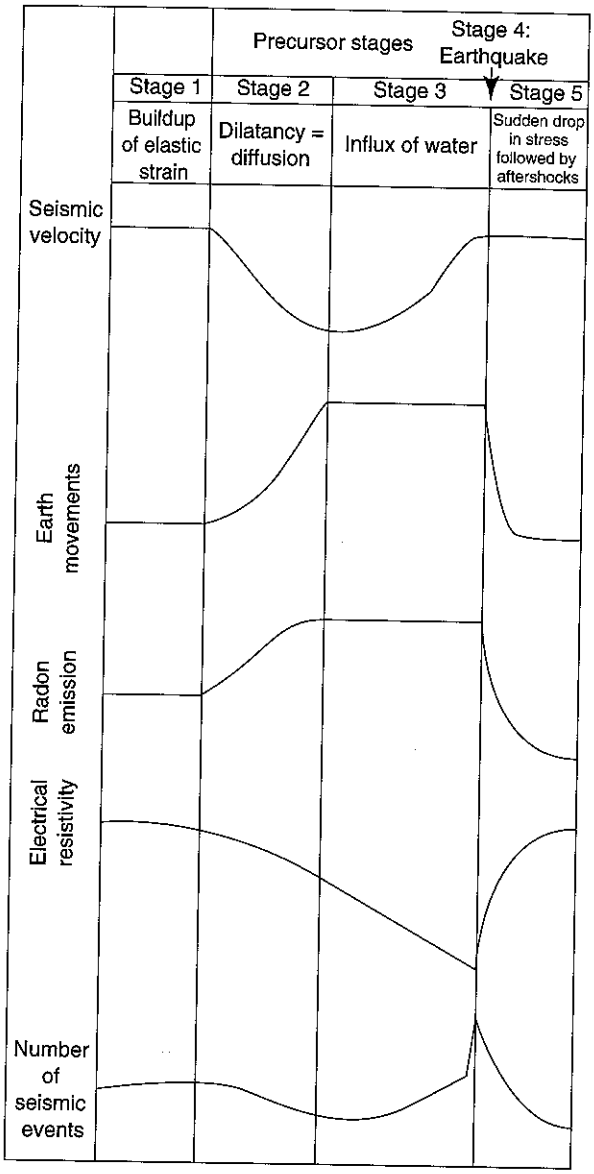

Figure 1.28 Dilatancy diffusion model to explain the mechanism responsible for triggering earthquakes. The curves show the expected precursory signals. (After Press, 1975. Scientific American, 232(5): 14–23. © May 1975 by Scientific American, Inc. All rights reserved.)

water is present. Deformation of the rocks and a variety of other processes are thought to increase the fluid pressure at depth, and this lowers the shear strength. If the fluid pressure becomes sufficiently high, then this can facilitate earthquakes. A wide variety of data from several environments, including subduction zones and active fold belts, suggest that high fluid pressures are present in many areas where earthquakes occur. Thus, there is increasing speculation and interest in the role of fluid flow that affects fault displacement and is intimately related to the earthquake cycle. This process has been termed the **fault-valve mechanism** [36, 37]. The mechanism is a hypothesis in which fluid pressure rises until failure occurs, thus triggering an earthquake and discharging fluid upward.

Subsequent sealing of the rock matrix in the fault zone allows fluid pressure to reaccumulate, initiating another cycle.

PREDICTING GROUND MOTION

Engineering design of critical facilities such as power plants and dams requires careful evaluation of earthquake hazard. Of particular importance is prediction of **strong ground motion** due to earthquakes that may occur at or near facility sites. Seismographs provide information about the amplitude of seismic shaking, as illustrated in Figure 1.10a. Instruments known as **accelographs** measure and record vertical and horizontal accelerations produced by earthquakes. By measuring the vertical and horizontal components of acceleration in both the north-south and east-west directions, a three-dimensional picture of ground acceleration is created [10]. Another important parameter is the duration of shaking. For ground accelerations measured from an accelograph, the duration of strong shaking is defined as the **bracketed duration**, which is the time in which the acceleration is above a minimum value, often 0.05 *g*. For the example shown on Figure 1.29, the duration of strong shaking is approximately 8 s.

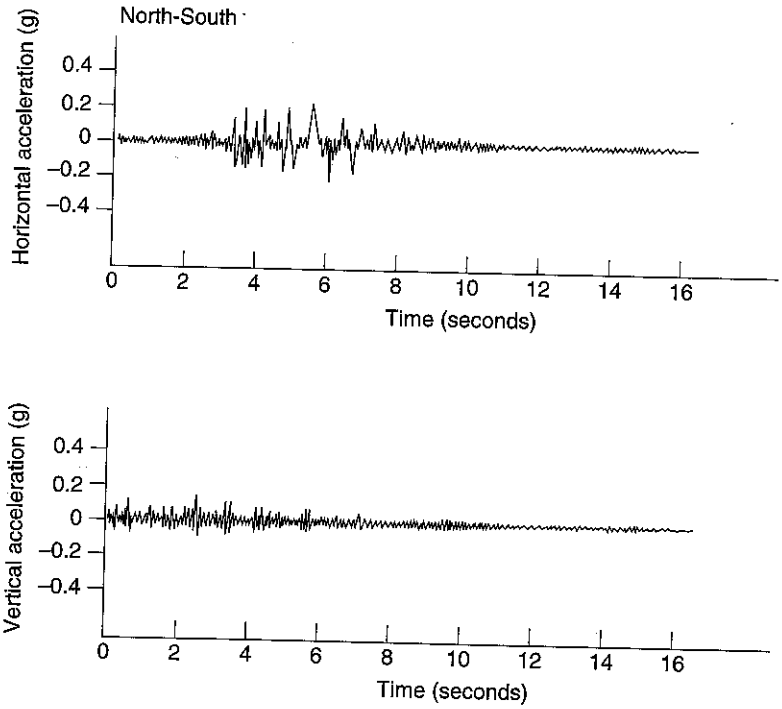

Figure 1.29 Hypothetical graph of vertical and horizontal accelerations from an earthquake with a magnitude M_W 6.5 at a distance of about 40 km from the center of energy release. Time "0" on the graph is the first arrival of the P waves. Vertical accelerations in this example are approximately 0.1 *g*. On the graph that shows the north-south horizontal acceleration, the S and L waves arrive approximately 4 s later than P waves with a maximum acceleration of approximately 0.25 *g*.

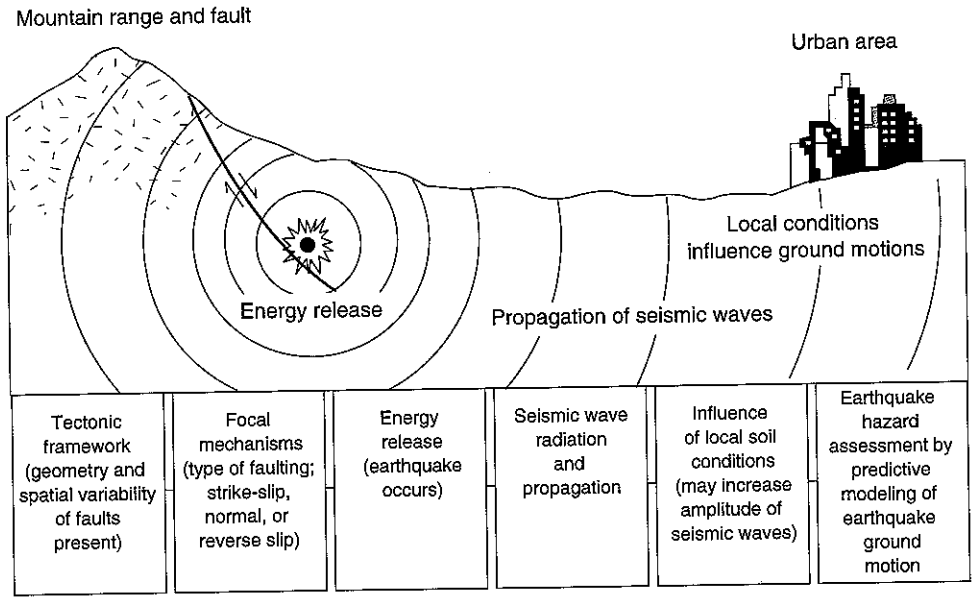

Figure 1.30 Assessment of earthquake hazard by modeling of ground motion. (After Vogel, 1988. In A. Vogel and K. Brandes (eds.), *Earthquake Prognostics*. Brannschweig/Weisbaden: Friedr. Vieweg & Sohn, 1–13.)

Assessment of earthquake hazard at a particular site starts with identification of the **tectonic framework** (geometry and spatial pattern of faults or seismic sources) in order to predict earthquake ground motion (Figure 1.30). Another major step in site assessment is to develop **time histories** (relationships between properties of seismic waves and time) of ground motion resulting from the largest earthquakes that could shake the site of interest. The process of predicting ground motion from a given earthquake may be illustrated by considering a hypothetical example. Figure 1.31 shows an example of a dam and reservoir site. The objective is to predict strong ground motion at the dam from several seismic sources (faults) in the area. The tectonic framework shown consists of a north-dipping reverse fault and an associated fold (an anticline) located to the north of the dam, as well as a right-lateral strike-slip fault located to the south of the dam. Figure 1.31b shows a cross section through the dam illustrating the geologic environment, including several different earth materials, folds, and faults. Assuming that earthquakes would occur at depths of approximately 10 km, the distances from the dam to the two seismic sources (the reverse fault and the strike-slip fault) are 42 km and 32 km, respectively. Thus, for this area, two focal mechanisms are possible: reverse faulting and strike-slip faulting.

The next step in the process is to estimate the largest earthquakes likely to occur on these faults. Assume that field work in the area revealed ground rupture and other evidence of faulting in the past, suggesting that on the strike-slip fault, approximately 50 km of fault length might rupture in a single event, with right-lateral strike-slip motion of 2 m. The field work also revealed that the largest rupture likely on the reverse fault would be 30 km of fault length, with vertical displacement of about 1 m. Given this in-

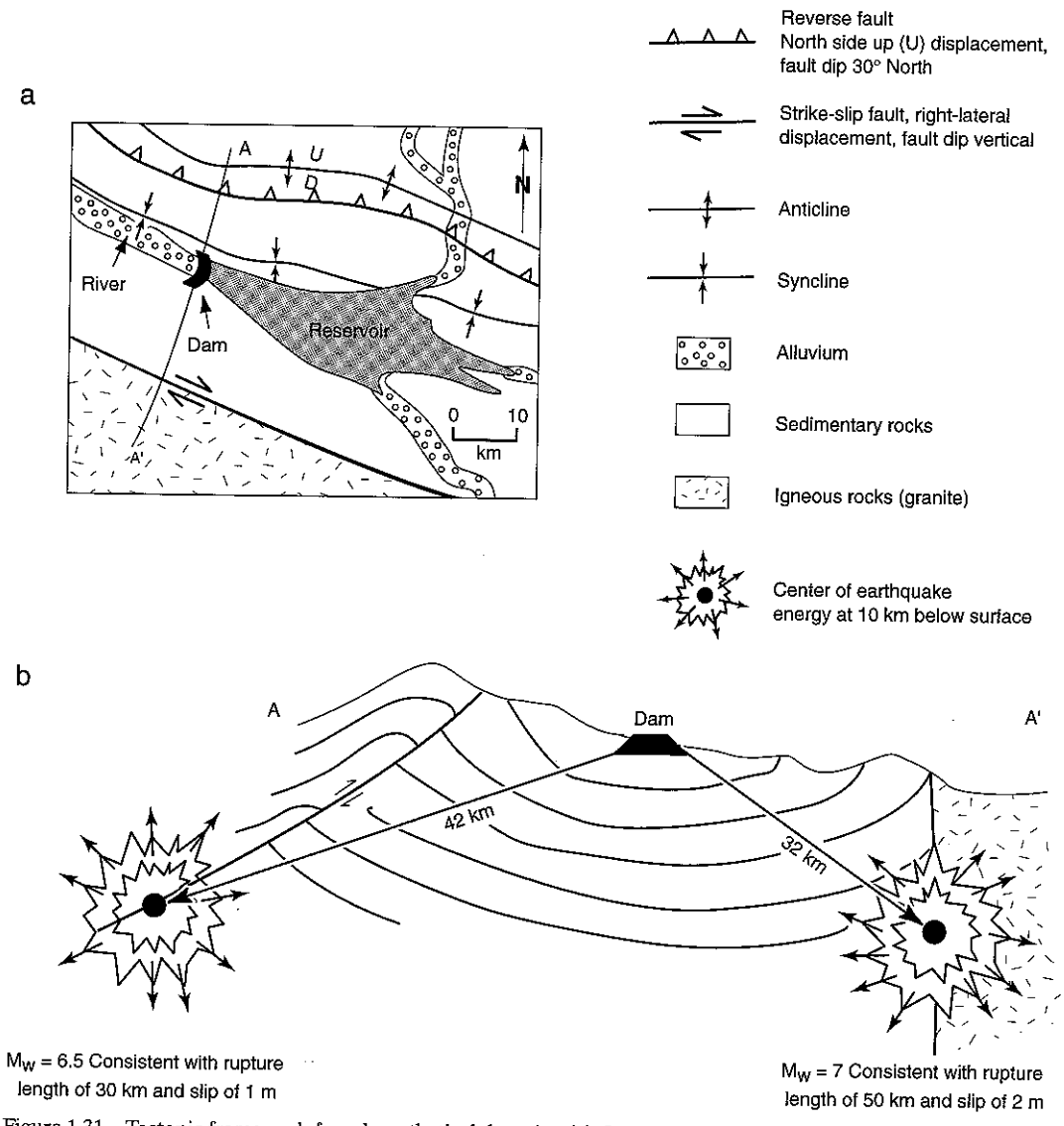

Figure 1.31 Tectonic framework for a hypothetical dam site. (a) Geologic map. (b) Cross section A-A', showing seismic sources and distances of possible ruptures to the dam.

formation, the magnitudes of possible earthquake events can be estimated from graphs such as those shown on Figure 1.32 [38, 39]. Fifty kilometers of surface rupture are associated with an earthquake of approximately M_W 7. Similarly, for the reverse fault with surface rupture length of 30 km, the magnitude of a possible earthquake is estimated to be M_W 6.5. Notice on Figure 1.32 that the regression line that predicts the moment magnitude is for strike-slip, normal, and reverse faults. Statistical analyses have suggested that the relation between moment magnitude and length of surface rupture is not sensitive to the style of faulting [39].

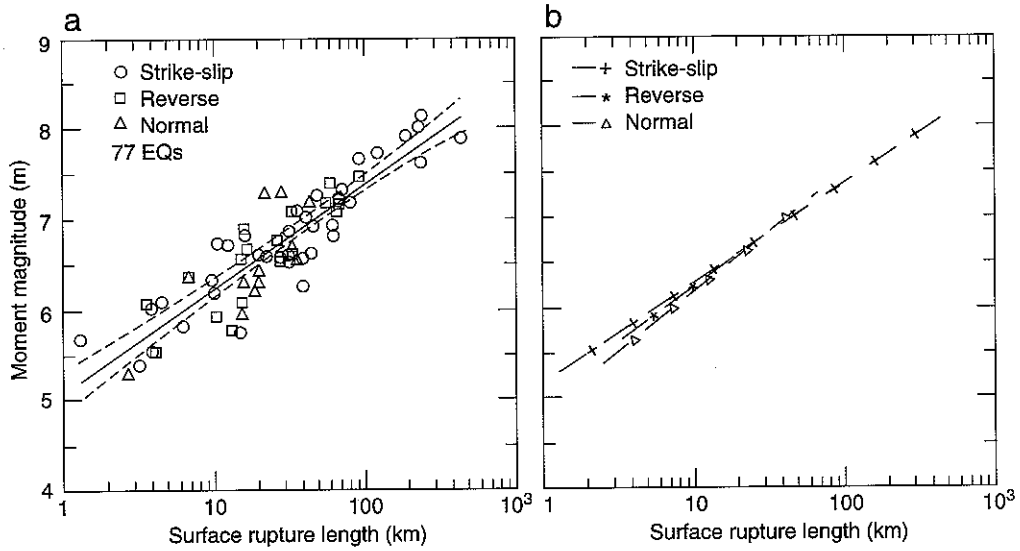

Figure 1.32 Relationship between moment magnitude of an earthquake and surface rupture length. Data for 77 events are shown in (a). Solid line is the "best-fit" or regression line, and dashed lines are error bars at the 95% confidence level. Graph in (b) shows individual lines for different types of faults. There is no significant difference between the lines. (After Wells and Coppersmith, 1994 [39].)

With the preceding information, the next task is to estimate the seismic shaking or ground motion expected from these events. These are referred to as **response spectra**, which are relationships between ground motion and period of earthquake waves [40]. There are two approaches available to estimate the response spectra: (1) empirical evaluation, and (2) simulation.

- Where ground motions have been recorded from previous events, **empirical evaluation** begins with identifying those records that most closely approach the conditions for the site of interest. The objective is to match as closely as possible the tectonic framework, rock types, type of faulting, and earthquake magnitude from a known event to known conditions at the site. The assumption is that the shaking and strong ground motion associated with a known earthquake will produce similar ground motion. Using our example of the dam site, an earthquake of M_W 6.4 on a reverse fault in Afghanistan might serve as a model for the reverse fault near the dam (Figure 1.31). Similarly, an earthquake of M_W 7.1 on the San Andreas fault in California may be used as a model to estimate the ground motion from such an event on the strike-slip fault. Of course, it is difficult to match exactly the conditions from a known event to those of the dam site, and so allowances are necessary to adjust for small differences in earthquake magnitude and distances to the predicted epicenters. If the match between a known event and possible event at the dam site is fairly good, then ground-motion parameters such as duration of shaking and average peak acceleration of ground motion may be estimated.

- The second approach is to develop theoretical or numerical models to estimate ground motions, including acceleration time histories for the various faulting scenarios [40, 41]. Such models are now commonly used in the seismic-risk evaluation of structures such as dams, bridges, and tall buildings.

Results from the modeling of ground motion are then compared with the empirical results and, if the agreement is good, the ground-motion parameters can be used to evaluate potential shaking, duration of shaking, and ground acceleration at the dam site. If this analysis is completed prior to the designing of a dam, then the parameters are useful to engineers designing the dam to minimize potential damage from earthquakes. If the evaluation is of an existing dam site, then the information is useful in evaluating whether additional engineering work is necessary to upgrade the structure to render it more resistant to earthquakes.

The preceding discussion of methods used to assess earthquake hazard outlines procedures for evaluating the seismic hazard at power plants, dams, and other critical facilities. Although this methodology suffers from limiting assumptions and shortcomings, it certainly is a valuable tool insofar as it allows estimation of strong ground motions likely to affect a particular site. As additional earthquake records are obtained and, in particular, strong ground motions close to the epicentral areas are recorded, then our understanding of how better to design structures to withstand earthquake shaking will improve.

SUMMARY

Tectonics refers to processes and landforms resulting from deformation of the Earth's crust, and active tectonics refers to those tectonic processes that produce deformation of the Earth's crust on a time scale that is significant to humans. Active tectonics includes slow disruption of the crust that may cause damage to human structures but it is most concerned with catastrophic events such as earthquakes that cause severe damage to people, property, and society.

A fault is a fracture or fracture system along which rocks have been displaced. A group of related faults or fault traces is known as a fault zone, and most major fault zones are segmented. Fault segments are recognized on the basis of changes in the fault-zone morphology or geometry as well as seismic and paleoseismic activity. Active fault zones are those for which it can be demonstrated that a fault has moved during the past 10 ky. Faults that have moved in the past 1.65 M.y. are considered potentially active, and those that have not moved during that period generally are classified as inactive.

Both magnitude and intensity of earthquakes are important in evaluating potential earthquake hazard. Although the Richter magnitude has been used for many years, it is now being replaced by the more physically based moment magnitude system. The Modified Mercalli Scale is based on observations concerning severity of shaking and response of structures to earthquakes. Effects of earthquakes include violent shaking, surface rupture, liquefaction, landslides, fires, tsunami, and regional changes in land elevation. Earthquakes also have been caused by human activities, such as reservoir construction, subsurface injection of liquid waste, and mining.

Estimation of seismic risk is an important endeavor and involves development of seismic risk maps and calculation of conditional probabilities of earthquakes occurring in the future. Slip rate on a fault is an important parameter in estimating the earthquake

hazard for a particular fault. The average recurrence interval of earthquakes on a particular fault also is an important characteristic and can be determined by paleoseismic data, the ratio of assumed displacement per event to the slip rate, and historical seismicity.

An important aspect of earthquake-hazard reduction is prediction of strong ground motion. Assessment of the earthquake hazard starts with identification of the tectonic framework (geometry and spatial pattern of faults or seismic sources) followed by identification of possible focal mechanisms for earthquakes on faults present in the area being evaluated. Field work and other evidence are used to predict the magnitude of earthquake events that might be expected at a particular site.

REFERENCES CITED

1. Geophysics Study Committee, 1986. Overview and recommendations. In *Active Tectonics*. Washington, DC: National Academy Press, 3–19.
2. Davis, G. H., 1993. Basic science planning initative in "active tectonics." *EOS: Transactions, American Geophysical* Union, 74(43):59.
3. White, G. F., and J. E. Haas, 1975. *Assessment of Research on Natural Hazards*. Cambridge, MA: MIT Press.
4. Advisory Committee on the International Decade for Natural Disaster Reduction, 1989. *Reducing Disaster's Toll*. Washington, DC: National Academy Press.
5. Le Pichon, X., 1968. Sea-floor spreading and continental drift. *Journal of Geophysical Research*, 73:3661–3697.
6. Isacks, B., J. Oliver, and L. Sykes, 1968. Seismology and the new global tectonics. *Journal of Geophysical Research*, 73:5855–5899.
7. Dewey, J. F., 1972. Plate tectonics. *Scientific American*, 226(5):56–68.
8. Hamilton, R. M., 1980. Quakes along the Mississippi. *Natural History*, 89(8):70–75.
9. Mueller, K., J. Champion, M. Guccione, and K. Kelson, 1999. Fault slip rates in the modern New Madrid Seismic Zone. *Science*, 286:1135–1138.
10. Bolt, B. A., 1993. *Earthquakes*. San Francisco: W. H. Freeman.
11. Hart, E. W., W. A. Bryant, and J. A. Treiman, 1993. Surface faulting associated with the June 1992 Landers earthquake, California. *California Geology*, 46:10–16.
12. Hanks, T. C., 1985. The national earthquake hazards reduction program: scientific status. *U.S. Geological Survey Bulletin* 1659.
13. Hays, W. W., 1981. Facing geologic and hydrologic hazards: earth science consideration *U.S. Geological Survey Professional Paper* 1240-B.
14. Jones, R. A., 1986. New lessons from quake in Mexico. *Los Angeles Times*, September 26.
15. Hough, S. E., P. A. Friberg, R. Busby, E. F. Field, K. H. Jacob, and R. D. Borcherdt, 1989. Did mud cause freeway collapse? *EOS: Transactions, American Geophysical Union*, 70:1497–1504.
16. U.S. Geological Survey Staff, 1996. U.S.G.S. response to an urban earthquake, Northridge '94. *U.S. Geological Survey Open File Report* 96–263.
17. Radbruch, D. H., B. J. Lennet, M. G. Bonilla, B. J. Lennert, F. B. Blanchard, G. L. Laverty, L. S. Cluff, and K. V. Steinbrugge 1966. Tectonic creep in the Hayward fault zone, California. U.S. Geological Survey Circular 525.
18. Steinbrugge, K. V., and E. G. Zacher, 1973. Creep on the San Andreas fault. In R. W. Tank (ed.), *Focus on Environmental Geology*. New York: Oxford University Press, 132–137.
19. Working Group on California Earthquake Probabilities, 1995. Seismic Hazards in Southern California: Probable earthquakes, 1994–2024. *Bulletin of the Seismological Society of America*, 85:379–439.

20. Toppozada, T. R., 1993. The Landers–Big Bear earthquake sequence and its felt effects. *California Geology* 46 (Jan.–Feb.):3–9.
21. U.S. Geological Survey, 1999. Special Report: The Hector Mine earthquake, 10/16/99. Accessed @ http://www.socal.wr.usgs.gov/hector/report/html
22. Working Group on California Earthquake Probabilities, 1999. Major quake likely to strike between 2000 and 2030. USGS Fact Sheet 152–99.
23. Office of Emergency Preparedness, 1972. *Disaster Preparedness*: 1, 3: Washington, DC.
24. Youd, T. L., D. R. Nichols, E. J. Helley, and K. R. Lajoie, 1975. Liquefaction potential. In R. D. Borcherdt (ed.), Studies for Seismic Zonation of the San Francisco Bay Region. *U.S. Geological Survey Professional Paper* 941: A68–A74.
25. Office of Emergency Preparedness, 1972. *Disaster Preparedness*: 1, 2: Washington, DC.
26. Hokkaido Tsunami Survey Group, 1993. Tsunami devastates Japanese coastal region. *EOS: Transactions of the American Geophysical Union*, 74:417–432.
27. Geist, E. L., 1998. Source characteristics of the July 17, 1998 Papua New Guinea tsunami. American Geophysical Union, Fall Meeting, Abstracts, p. F571.
28. Koenig, R. 2001. Researchers target deadly tsunamis. *Science*, 293:1251-1253..
29. Slemmons, D. B., and C. M. DePolo, 1986. Evaluation of active faulting and associated hazards. In *Active Tectonics*. Washington, DC: National Academy Press, 45–62.
30. Hansen, W. R., 1965. The Alaskan earthquake, March 27, 1964: Effects on communities. *U. S. Geological Survey Professional Paper* 542-A.
31. Oppenheimer, D., G. Beroza, G. Carver, L. Dengler, J. Eaton, L. Gee, F. Gonzales, A. Jayko, W. H. Li, M. Lisowski, M. Magee, G. Marshall, M. Murray, R. McPherson, B. Romanowicz, K. Satake, R. Simpson, P. Somerville, R. Stein, and D. Valentine, 1993. The Cape Mendocino, California, earthquakes of April 1992: subduction at the triple junction. *Science*, 261:433–438.
32. Pakiser, L. C., J. P. Eaton, J. H. Healy, and C. B. Raleigh, 1969. Earthquake prediction and control. *Science*, 166:1467–1474.
33. Evans, D. M., 1966. Man-made earthquakes in Denver. *Geotimes*, 10(9):11–18.
34. Sylvester, A. G., and J. Heinemann, 1996. Preseismic tilt and triggered reverse faulting due to unloading in a diatomite quarry near Lompoc, California. *Seismological Research Letters*, 67(6):11–18.
35. Press, F., 1975. Earthquake prediction. *Scientific American*, 232(5):14–23.
36. Sibson, R. H., 1981. Fluid flow accompanying faulting: field evidence and models. In D. W. Simpson and P. G. Richards (eds.), *Earthquake Prediction, an International Review*. M. Ewing Series 4. Washington, DC: American Geophysical Union, 593–603.
37. Keller, E. A., and H. A. Loaiciga, 1993. Fluid-pressure induced seismicity at regional scales. *Geophysical Research Letters*, 20:1683–1686.
38. Slemmons, D. B., 1982. Determination of design earthquake magnitudes for microzonation. In M. Sherif (ed.), *Proceedings: 3rd International Earthquake Microzonation Conference*. Washington, DC: U.S. National Science Foundation, 119–130.
39. Wells, D. L., and K. J. Coppersmith, 1994. New empirical relationships among magnitude, rupture length, rupture width, rupture area and surface displacement. *Bulletin of the Seismological Society of America*, 84:974–1002.
40. Auersch, L., 1988. Seismic response of three-dimensional structures using a Green's function approach to the soil. *In* A. Vogel and K. Brandes (eds.), *Earthquake Prognostics*. Brannschweig/Weisbaden: Friedr. Vieweg & Sohn, 393–403.
41. Damrath, R., 1988. Modal response analysis of structures. *In* A. Vogel and K. Brandes (eds.), *Earthquake Prognostics*. Brannschweig/Weisbaden: Friedr. Vieweg & Sohn, 405–426.